Asia Pac. J. Math. 2023 **10**:10

ANALYSIS OF COVID-19 DISEASE WITH CARELESS INFECTIVE USING SEITRS MODEL

OLUWOLE DANIEL MAKINDE[1], ADETAYO SAMUEL EEGUNJOBI[2,*]

[1]Faculty of Military Science, Stellenbosch University, Private Bag X2, Saldanha 7395, South Africa

[2]Mathematics Department, Namibia University of Science and Technology, Windhoek, Namibia

*Corresponding author: samdet1@yahoo.com

Received Feb. 27, 2023

Abstract. The COVID-19 pandemic has had a significant impact on the global population, with millions of cases and deaths reported worldwide. In this study, we use mathematical models to analyze the spread of the disease, with a focus on careless infective models. We develop and analyze mathematical models to understand the transmission dynamics of COVID-19 , taking into account the impact of human behavior, such as the spread of the disease by individuals who are unaware that they are infected. Our results provide insights into the role of careless infective individuals in the spread of the disease and suggest the need for targeted interventions to reduce the impact of COVID-19 The results of this study contribute to a better understanding of the spread of COVID-19 and inform public health measures to control its transmission.

2020 Mathematics Subject Classification. 92D30.

Key words and phrases. COVID-19 disease; careless infective; SEITRS model; qualitative analysis; numerical simulation

1. Introduction

The COVID-19 pandemic has had a profound effect on the world, leading to widespread illness and death, and causing major disruptions to global economies and societies. One of the key factors in the spread of the disease is the behavior of infected individuals, particularly those who are unaware that they are infected and continue to spread the virus to others. The infection's severity can vary from mild to severe, with potential complications that include pneumonia, acute respiratory distress syndrome, and even death. To better understand the

DOI: 10.28924/APJM/10-10

impact of such behavior on the transmission dynamics of COVID-19 , it is crucial to incorporate it into mathematical models of the disease.

There have been a number of studies conducted on the transmission and dynamics of COVD-19. An SEIARD mathematical model was proposed by [1] in order to investigate the recent outbreak of the coronavirus disease known as COVID-19 in Mexico. They estimate the per day infection, death, and recovery rates, as well as the basic reproduction number (R_0), using the next-generation matrix method. In terms of R_0, the local stability of the disease-free equilibrium was determined to have been established. [2] formulated a six compartmental epidemiological deterministic model for the transmission dynamics of two strains of COVID-19 diseases in a given community with quarantine and recovery as a result of treatment. A qualitative analysis of the model was carried out by utilizing the stability theory of differential equations. The basic reproduction number, R_0 was calculated for both strains, and the sensitivity index of the parameters was investigated. [3] investigated the effect that a variety of non-pharmaceutical control measures had on the population dynamics of the novel coronavirus disease 2019 (COVID-19). They developed a mathematical model by making use of the information that was readily available, with the goal of creating a tool that could make predictions regarding the total number of cases that have been reported and the total number of cases that are currently being investigated. They were able to estimate the basic reproduction number of the disease outbreak of the model. They demonstrated the impact that the control measures had on the dynamics of COVID-19 by using numerical simulations as their primary tool. Ordinary Differential Equation (ODE) and Fractional Differential Equation were both components of the mathematical model that [4] used to describe the outbreak of Coronavirus Disease 2019 (COVID-19). They took into account both asymptomatic and symptomatic infected individuals, the fact that an exposed individual is either placed in quarantine initially or moved to one of the classes of infected individuals, with the possibility that a susceptible individual could also move directly to the quarantined class. They carried out the sensitivity analysis on the parameters found in the R_0 to demonstrate the progression of the disease. They proceeded to carry out the numerical solution of the fractional model by utilizing the Atangana-Toufik numerical scheme.

The [5]- [8] have studied the selection of interventions could be of helped along by dynamic analyses and model-based predictions. [9] developed an epidemiological model that consisted of five different compartments by basing it on the observed characteristics of transmission.They

carried out the research and came to the conclusion that SARS-CoV-2 has a high rate of transmission between people in their middle years and those in their later years, while children have a very low risk of contracting COVID-19.

[10] presented a compartmental mathematical model with the intention of predicting and controlling the transmission dynamics of the COVID-19 pandemic in India using epidemiological data that was already available. They computed the basic reproduction number, which was then utilized in the subsequent research on the model simulations and predictions. They carried out local and global stability analysis for the infection-free equilibrium point as well as an endemic equilibrium point. The simulation of their model demonstrates that the disease transmission rate as defined in their model is more effective in reducing the fundamental reproduction number. Using computer simulation models is one technique to investigate the consequential expansion of these lethal eruptions. The results of SIR, SEIR, and SEIRD models are carried out in a variety of papers using a variety of numerical and analytical methodologies. In addition to helping us understand how epidemic diseases behave over time, numerical methods can help us take more effective preventative actions. [11] employed a mathematical compartmental model of the pandemic behavior of COVID-19 in Wuhan, China.The system of ordinary differential equations was solved using the Adams-Bashforth predictor-corrector technique, which relies on Lagrange polynomials. Numerical simulations were run, and the model's sensitivity was analyzed. The dynamical behavior of a COVID-19 infection was modeled by [12] using isolation class. By demonstrating the model's positivity, local stability, and global stability, they presented their findings. For performing the numerical simulation, they used the Runge-Kutta method with a fourth-order accuracy and a nonstandard finite difference (NSFD) scheme.

[16] categorized people as being hyper-susceptible and developed a mathematical model to study the effect that hyper-susceptibility has on the dynamics of an Ebola virus disease outbreak. Based on their findings, they predicted global stability for the disease-free equilibrium point when the basic reproduction number is greater than one. In addition to this, They demonstrated that the model exhibited forward bifurcation, which hints at the possibility of eradication by maintaining a value below unity. Furthermore, it was demonstrated that the rate of disease transmission is extremely sensitive to contact rate, transmission probability, death rate, and hyper-susceptibility. [17] formulated the dynamic transmission model of the

two strains super-infection of dengue virus, carried out the mathematical analysis on the dynamics transmission and performed the numerical simulation of the model. A mathematical model for Pneumonia–Typhoid co-infection was proposed and analyzed by [18] in order to investigate the characteristic relationship between the two diseases as a result of preventative and treatment strategies. The basic reproduction number is estimated by taking into account the stability of equilibria and existence. They derived the necessary conditions for the optimal control and optimality system by applying Pontryagin's maximum principle. The optimality system is numerically simulated by taking into consideration four different strategies, and the effectiveness of each of these strategies in terms of cost is analyzed. They discovered that the cost of treating pneumonia along with preventing typhoid fever was the lowest. [19] modeled and analyzed the disease caused by the Ebola virus, which had a non-linear incidence rate. They carried out an uncertainty analysis on the basic reproductive number in order to quantify its sensitivity to other disease-related parameters. They also analyzed the sensitivity of the final epidemic size to the time control interventions and provide the combination of the interventions that is most cost effective. [20] constructed and analyzed a nonlinear mathematical model for pneumonia transmission dynamics in varied populations. Stability theory of differential equations was used to study deterministic compartmental model. The effective reproduction number and asymptotic stability criteria for disease-free and endemic equilibria are determined. The model's bifurcation and the basic reproduction number's sensitivity indices to important factors are determined. Three control solutions solve Pontryagin's maximal principle's optimal control problem. Prevention and treatment were found to be the most cost-effective pneumonia pandemic control techniques.

Research has shown that unintentional spread of Covid-19 can play a major role in the early stages of a pandemic due to careless infected individuals. This study will result in the construction of a mathematical model in which the interaction of the exposed population, the careless population, and the careful population will be examined. We estimate the basic reproduction number of the model. The positivity, boundedness, and both local and global asymptomatic stability of the model are discussed. The sensitivity and bifurcation analyses are carried out, and we simulate numerically and present the graphical solution to show the effect of some varied parameters.

2. Model Problem

The spread of COVID-19 with careless infective will be modeled using a compartmental differential equation here. The dynamics of six subpopulations are tracked by the model. These subpopulations are: susceptible $(S(t))$, exposed $(E(t))$, careless infective (not screen and isolated) $(I_c(t))$, careful infective (screen and isolated) $(I_r(t))$, treated $(T(t))$ and recovered $(R(t))$. In the process of developing the model, the following assumption will be taken into consideration: in the population, the susceptible and infected are homogeneous; at the beginning of the outbreak of COVID-19, there were no efforts taken to intervene in any way and put a stop to its spread and birth are allowed into the population.

The susceptible population can increase due to the birth and recovery and decrease by natural death and after an infection, a trait that has been picked up as a result of contact with an infected individual. $\beta_1 I_c$ and $\beta_2 I_r$ are transmission coefficients. Exposed subpopulation mimic the latent period and this refers to the time that passes between a human becoming infected with the virus and the point at which they are able to pass the virus on to other people who are susceptible. The individuals in the exposed compartment have the disease but are not contagious; in other words, they are unable to pass it on to others. This compartment decreases with rate τ and become infectious and probability ρ to become careless infection or $(1-\rho)$ to become careful infective. The careless infective are gotten from exposed compartment with rate rho and goes to treatment with rate ϕ_1 or death either by natural μ or careless disease death γ_1. The careful infective compartment is obtained from an exposed compartment at a rate $(1-\rho)$, and then goes treatment at the rate ϕ_2 or dies as a result of natural death μ or careless disease death γ_2.

Treatment compartment is obtained from both careless infective anf careful infective compartments with rate ϕ_1 and ϕ_2. There is tendency for natural death μ and death rate of infective under treatment γ_3 in this compartment. The treatment compartment also decreases with recovery rate ϵ. All individual that are infected moves to recovered compartment with rate ϵ. Individual in the recovery compartment can move to susceptible with α or die naturally.

Hence, the system of differential equations that will model the dynamics spread of the considering situations are given below:

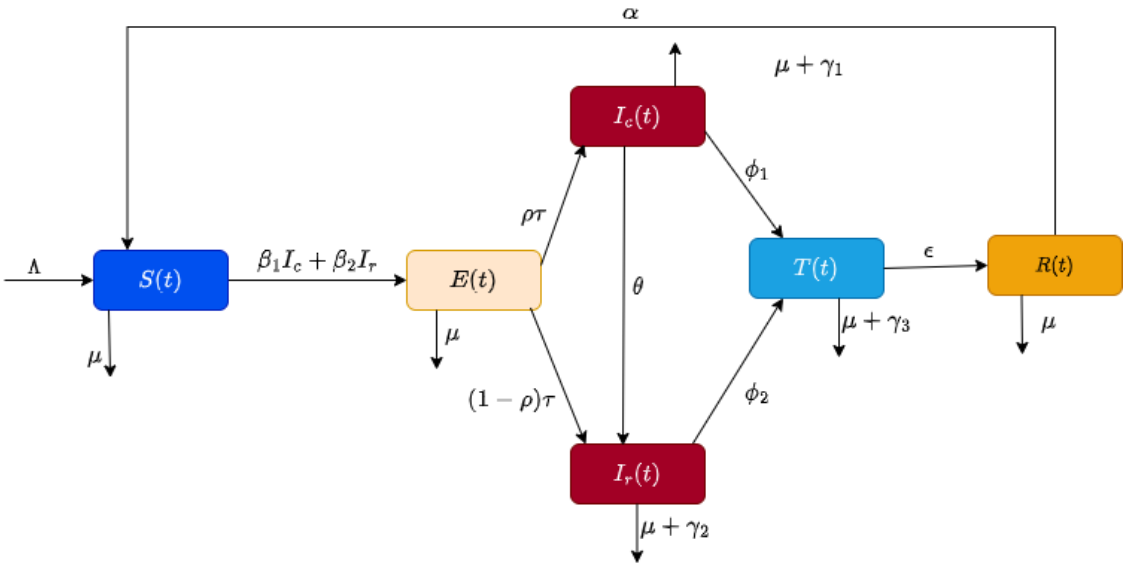

FIGURE 1. Schematic diagram depicting the transmission dynamics of model

$$
\begin{aligned}
\frac{dS(t)}{dt} &= \Lambda-(\beta_1 I_c+\beta_2 I_r)S(t)+\alpha R(t)-\mu S(t),\\
\frac{dE(t)}{dt} &= (\beta_1 I_c+\beta_2 I_r)S(t)-(\tau+\mu)E(t),\\
\frac{dI_c(t)}{dt} &= \rho\tau E(t)-(\phi_1+\theta+\gamma_1+\mu)I_c,\\
\frac{dI_r(t)}{dt} &= (1-\rho)\tau E(t)+\theta I_c-(\gamma_2+\phi_2+\mu)I_r,\\
\frac{dT(t)}{dt} &= \phi_1 I_c+\phi_2 I_r-(\gamma_3+\epsilon+\mu)T(t),\\
\frac{dR(t)}{dt} &= \epsilon T(t)-(\alpha+\mu)R(t)
\end{aligned}
\tag{1}
$$

with initial conditions

$$S(0)=S_0, E(0)=E_0, I_c(0)=I_{c0}, I_r(0)=I_{r0}, T(0)=T_0, R(0)=R_0$$

where

$$N(t)=S(t)+E(t)+I_c(t)+I_r(t)+T(t)+R(t).$$

Variables & Parameters	*Description*
$S(t)$	Susceptible
$E(t)$	Exposed
$I_c(t)$	Careless infective (not Screen and Isolated)
$I_r(t)$	Careful infective (Screened & Isolated)s
$T(t)$	Treatment
$R(t)$	Recovered
β_1	Transmission rate with careless infectives
β_2	ITransmission rate with careful infective
α	Conversion rate of recovered to susceptible
Λ	Recruitment rate (birth or immigration)
θ	Conversion rate of careless to careful infective
μ	Natural death rate
ρ	Rate of becoming careless infective
τ	Conversion rate of exposed to infective
γ_1	Death rate of careless infectivee
γ_2	Death rate of careful infective e
γ_3	Death rate of infective under treatment
ϕ_1	Treatment rate of careless infective
ϕ_2	Treatment rate of careful infective
ϵ	Recovery rate after treatment

TABLE 1. Description of variables and parameters

3. THE MODEL BASIC PROPERTIES

3.1. **Positivity and Boundeddness.** It is essential to demostrate that all of the model's variables for (1) are npn-negative for any time $t > 0$ and alsp bounded.

Theorem 3.1. Suppose the model (1) starting conditions are

$$S(0) \geq 0, E(0) \geq 0, I_c(0) \geq 0, I_r(0) \geq 0, T(0) \geq 0, R(0) \geq 0$$

the the model (1) has positive $S(t), E(t), I_c(t), I_r(t), T(t), R(t)$ solutions for all time $t > 0$.

Proof. In order to demonstrate that the solutions have a positive solutions, we shall employ the first equation in (1).

Let

$$t_a = \sup\{t > 0 : S > 0, E > 0, I_c > 0, I_r > 0, T > 0, R > 0\} \in [0, t].$$

For $t > 0$, the we have

$$\frac{dS(t)}{dt} = \Lambda - (\beta_1 I_c(t) + \beta_2 I_r(t))S(t) + \alpha R(t) - \mu S(t) \geq \Lambda - (u(t) + \mu)S(t)$$

where $u(t) = \beta_1 I_c(t) + \beta_2 I_r(t)$ This implies

$$\frac{dS(t)}{dt} \geq \Lambda - (u(t) + \mu)S(t)$$

Integrating factor allows us to achieve the following

$$\frac{d}{dt}\left[S(t)e^{\mu t + \int_0^t u(p)dp}\right] \geq \Lambda e^{\mu t + \int_0^t u(p)dp}$$

Having solved and integrated both sides from 0 to t_a, we have the following

$$S(t_a) \geq S(0)e^{-\{\mu t_a + \int_0^{t_a} u(p)dp\}} + e^{-\{\mu t_a + \int_0^{t_a} u(p)dp\}} \times \int_0^{t_a} \Lambda e^{\mu t + \int_0^t u(p)dp} > 0 \tag{2}$$

As a direct consequences of this, we are able to deduce that $S(t) > 0$. Using the same line of reasoning, we can also demonstrate that $E(t), I_c(t), I_r(t), T(t)$ and $R(t)$ are all strictly greater than zero. □

3.2. **Boundeddness.** In epidemic models, the concept of boundednesss of the solution refers to determining whether or not the model's solutions fall inside a predetermined range of values.

Theorem 3.2. Every solution of the equation (1) has an upper and lower limit if $\lim_{t\to\infty} \sup N(t) \leq \frac{\Lambda}{\mu}$, therefore

$$N(t) = S(t) + E(t) + I_c(t) + I_r(t) + T(t) + R(t).$$

Proof. Summing up all the equation in model (1), we obtain

$$\frac{dN(t)}{dt} = \Lambda - \mu N(t) - (\gamma_1 I_c(t) + \gamma_1 I_r(t) + \gamma_3 T(t)) \leq \Lambda - \mu N(t) \tag{3}$$

This implies that

$$\frac{dN(t)}{dt} + \mu N(t) \leq \Lambda \tag{4}$$

Applying integrating factor $e^{\mu t}$ and afer solving we obtain

$$N(t) \leq \frac{\Lambda}{\mu} + N_0 e^{-\mu t}, \quad \text{where} \quad N_0 = N(0)$$

Now as t goes to ∞, we have

$$\limsup_{t\to\infty} N(t) \leq \frac{\Lambda}{\mu}. \tag{5}$$

As a result of (5), we have established tha the model (1) is bounded.

□

3.3. **The basic reproduction number.**

$$\mathcal{F} = \begin{bmatrix} (\beta_1 I_c + \beta_2 I_r)S \\ 0 \\ 0 \end{bmatrix}, \quad \mathcal{V} = \begin{bmatrix} (\tau+\mu)E \\ -\rho\tau E + (\phi_1+\theta+\gamma_1+\mu)I_c \\ -(1-\rho)\tau E - \theta I_c + (\gamma_2+\phi_2+\mu)I_r \end{bmatrix}$$

Equation (1) has disease free equilibrium $E_0 = (\frac{\Lambda}{\mu}, 0, 0, 0, 0, 0)$. The Jacobian of $\mathcal{F}$ and $\mathcal{V}$ at E_0 are

$$F = \begin{bmatrix} 0 & \frac{\beta_1\Lambda}{\mu} & \frac{\beta_2\Lambda}{\mu} \\ 0 & 0 & 0 \\ 0 & 0 & 0 \end{bmatrix} \quad \mathcal{V} = \begin{bmatrix} \tau+\mu & 0 & 0 \\ -\rho\tau & \phi_1+\theta+\gamma_1+\mu & 0 \\ -(1-\rho)\tau & -\theta & \gamma_2+\phi_2+\mu \end{bmatrix}$$

and the inverse of V is

$$V^{-1} = \begin{bmatrix} \frac{1}{\tau+\mu} & 0 & 0 \\ \frac{\rho\tau}{(\tau+\mu)(\phi_1+\theta+\gamma_1+\mu)} & \frac{1}{\phi_1+\theta+\gamma_1+\mu} & 0 \\ -\frac{\tau(\mu\rho+\rho\gamma_1+\rho\phi_1-\mu-\theta-\gamma_1-\phi_1)}{(\tau+\mu)(\phi_1+\theta+\gamma_1+\mu)(\gamma_2+\phi_2+\mu)} & \frac{\theta}{(\phi_1+\theta+\gamma_1+\mu)(\gamma_2+\phi_2+\mu)} & \frac{1}{\gamma_2+\phi_2+\mu} \end{bmatrix}.$$

$$FV^{-1} = \begin{bmatrix} \frac{\beta_1\Lambda\rho\tau}{\mu(\tau+\mu)(\phi_1+\theta+\gamma_1+\mu)} - \\ \frac{\beta_2\Lambda\tau(\mu\rho+\rho\gamma_1+\rho\phi_1-\mu-\theta-\gamma_1-\phi_1)}{\mu(\tau+\mu)(\phi_1+\theta+\gamma_1+\mu)(\gamma_2+\phi_2+\mu)} & \frac{\beta_1\Lambda}{\mu(\phi_1+\theta+\gamma_1+\mu)} + \frac{\beta_2\Lambda\theta}{\mu(\phi_1+\theta+\gamma_1+\mu)(\gamma_2+\phi_2+\mu)} & \frac{\beta_2\Lambda}{\mu(\gamma_2+\phi_2+\mu)} \\ 0 & 0 & 0 \\ 0 & 0 & 0 \end{bmatrix}$$

The matrix, FV^{-1}, which is non-negative, is the next generation matrix of equations (1). The basic reproduction number that corresponds to this is

$$\begin{aligned} R_0 = \rho(FV^{-1}) = {} & \frac{\Lambda\rho\tau\beta_1}{\mu\left(\phi_1+\theta+\gamma_1+\mu\right)\left(\mu+\tau\right)} \\ & + \frac{\Lambda\tau\beta_2}{\mu\left(\phi_2+\gamma_2+\mu\right)\left(\mu+\tau\right)}\left[1 - \frac{\rho\left(\mu+\phi_1+\gamma_1\right)}{\left(\phi_1+\theta+\gamma_1+\mu\right)}\right] \end{aligned}$$

3.4. **Local Asymptotic stability of the model at disease free equilibrium(DFE).** The DFE, E_0 of the model (1) is a stated above.

Theorem 3.3. The disease free-equilibrium , E_0, is locally asymptotically stable if $R_0 < 1$, and unstable if $R_0 > 1$. .

Proof. The Jacobiam matrix of the first-five equations in the model (1) is evaluated at disease free equilibrium E_0 and this allow us to analyse the local stability of the model.

$$J(E_0) = \begin{bmatrix} -\mu & 0 & -\frac{\beta_1\Lambda}{\mu} & \frac{\beta_2\Lambda}{\mu} & 0 \\ -\beta_2 & -\tau-\mu & \frac{\beta_1\Lambda}{\mu} & 0 & 0 \\ 0 & \rho\tau & -\phi_1-\theta-\mu-\gamma_1 & 0 & 0 \\ 0 & \tau(1-\rho) & \theta & -\phi_2-\mu-\gamma_2 & 0 \\ 0 & 0 & \phi_1 & \phi_2 & -\epsilon-\mu-\gamma_3 \end{bmatrix}$$

The eigenvaluses of the matrix $J(E_0)$ are:

$$\lambda_1 = -\mu, \quad \lambda_2 = -(\tau+\mu)$$

$$\lambda_3 = -\frac{\mu^2(\mu+\theta+\phi_1+\gamma_1)(\tau+\mu) - \Lambda\rho\tau\beta_1(\mu+\beta_2)}{(\tau+\mu)\mu^2}, \quad \lambda_5 = -(\epsilon+\mu+\gamma_3)$$

$$\lambda_4 = -\frac{H - \mu^2(\mu+\gamma_2+\phi_2)(\mu+\theta+\phi_1+\gamma_1)(\tau+\mu)}{\Lambda\rho\tau\beta_1(\mu+\beta_2) - \mu^2(\mu+\theta+\phi_1+\gamma_1)(\tau+\mu)}$$

where

$$H = \Lambda\left(((\mu+\gamma_1+\phi_1)\rho - \mu - \gamma_1 - \theta - \phi_1)\beta_2^2 + \rho\beta_1(\mu+\gamma_2+\phi_2)\beta_2 + \mu\rho\beta_1(\mu+\gamma_2+\phi_2)\right)\tau$$

Due to the fact that all the eigenvalues are negative, then $R_0 < 1$ and therefore implies local asymptotically stabiliity. The basic reproduction number denoted by R_0, is a critical parameter in the model (1). It reflects the average number of new infections generated by a single infectious individual in a fully susceptible population where control measures are in effect. This number takes into consideration both careful and careless individuals, and represents the impact of an infected individual on the spread of the virus in the population. The value of R_0 is used to assess the effectiveness of control measures and guide decision-making regarding the public health response to the pandemic. Understanding and monitoring R_0 is crucial for effectively controlling the spread of COVID-19 and reducing its impact on public health. According to the theorem 2.1, the disease can be removed from the population iwhen $R_0 < 1$. □

3.5. **Global Asymptotic stability of the model at disease free equilibrium(DFE).**

Theorem 3.4.

- If $R_0 \leq 1$ the model (1) is global asymptotically stable
- If $R_0 > 1$ the model (1) is global asymptotically unstable in $U = \{(S, E, I_c, I_r, T, R) \in \mathbb{R}^6_+ : S + E + I_c + I_r + T + R\}$

Proof. W e assume $X = (E, I_c, I_r)^T$, such that

$$\frac{dX}{dt} \leq (F - V)X,$$

whre F and V are matrices obained in section (2.1). Suppose further that a is an eigenvector of F, $R_0 = \text{spectral}(FV^{-1}) = \text{spectral}(V^{-1}F)$. Suppose

$$V^{-1}F = R_0, \quad \text{then} \quad aV^{-1}F = R_0 a.$$

We assume the Lyapunov function as $\mathcal{L}_f = aV^{-1}X$.

$$\frac{d\mathcal{L}_f}{dt} = aV^{-1}\frac{dX}{dt} = aV^{-1}(F - V)X = (aV^{-1}F - a)X$$

This implies

$$\frac{d\mathcal{L}_f}{dt} = a(R_0 - 1)X$$

If $R_0 \leq 1$, this will implies tha $\frac{d\mathcal{L}_f}{dt} = 0$, so that $aX = 0$. Since $a > 0$, then $X = 0$, which means $E = I_c = I_r = 0$. If $R_0 < 1$, then

$$\frac{dE}{dt} + \frac{dI_c}{dt} + \frac{dI_r}{dt} = 0$$

and this gives

$$(S\beta_1 - \mu - \gamma_1 - \phi_1)I_c + (S\beta_2 - \mu - \gamma_2 - \phi_2)I_r + \mu E = 0$$

This implies

$$(S\beta_1 - \mu - \gamma_1 - \phi_1)I_c = 0 \quad \text{with} \quad E = I_r = 0$$

Hence

$$(\mu + \gamma_1 + \phi_1)\left[\frac{(\mu + \gamma_1 + \phi_1 + \theta)}{\rho\tau(\mu + \gamma_1 + \phi_1)}R_0 - 1\right] = 0$$

It is clearly seen that if $R_0 < 1$, then $\frac{d\mathcal{L}_f}{dt} < 0$. Otherway round,

$$(S\beta_2 - \mu - \gamma_2 - \phi_2)I_r = 0 \quad \text{with} \quad E = I_c = 0$$

then

$$(\mu+\gamma_2+\phi_2)\left[\frac{(\mu+\gamma_2+\phi_2)(\mu+\tau)}{(\mu+\gamma_2+\phi_2)\tau\left(1-\frac{\rho(\mu+\phi_1+\gamma_1)}{\phi_1+\theta+\gamma_1+\mu}\right)}R_0-1\right]=0$$

It is clearly seen that if $R_0<1$, then $\frac{d\mathcal{L}_f}{dt}<0$. This serves as evidence of the model's (1) global asymptotic stability.

On the other hand, if $R_0<1$, then it follows , based on the continuity of the vectir fields, that $\frac{d\mathcal{L}_f}{dt}>0$ in the vicinity of the U, according to the Lyapunov stability theory, the model (1) is therefore unstable. □

3.6. **Sensitivity Analysis.** This i evaluate the impact of change in input variable on the output of the model. The purpose of sensitivity analysis is to identify which inputs have the greatest effect on the output, and to quantify the extent of this effect. Estimates of the reproduction number sensitive indices are presented here.

Proposition:1 β_1,β_2,τ and ρ increase the basic reproduction number

Proof. This is due to the fact that when the basic reproduction number is differentiated with respect to each of the parameters, we get the following results:

$$\frac{\partial R_0}{\partial\beta_1}>0,\quad \frac{\partial R_0}{\partial\tau}>0,\quad \frac{\partial R_0}{\partial\rho}>0,\quad \text{and}\quad \frac{\partial R_0}{\partial\beta_2}>0.$$

□

Proposition:2 $\mu,\theta,\phi_1,\phi_2,\gamma_1$ and γ_2 idecrease the basic reproduction number

Proof. This is due to the fact that when the basic reproduction number is differentiated with respect to each of the parameters, we get the following results:

$$\frac{\partial R_0}{\partial\mu}<0,\quad \frac{\partial R_0}{\partial\theta}<0,\quad \frac{\partial R_0}{\partial\phi_1}<0,\quad \frac{\partial R_0}{\partial\phi_2}<0,\quad \frac{\partial R_0}{\partial\gamma_1}<0,\text{and}\quad \frac{\partial R_0}{\partial\gamma_2}<0.$$

□

The normalized forward sensitivity indices [2] are utilized in the computation of the sensitivity indices, which are obtained by

$$\Upsilon_L^{R_0}=\frac{\partial R_0}{\partial L}\times\frac{L}{|R_0|},$$

where L identifies the parameter for which the sensitivity index is calculated. The value 1 represents the greatest possible extent of the magnitude of $\Upsilon_L^{R_0}$. If the magnitude is 1, this indicates that an increase of $k\%$ in L will also result in an increase of $k\%$ in R_0. Likewise, if L decreases by $k\%$, then R_0 will also decrease by $k\%$. On the other hand, the smallest possible

number for $\Upsilon_L^{R_0}$ is -1. This suggests that an increase in L by $k\%$ will result in a corresponding decrease in R_0 by $k\%$, and a decrease in L by $k\%$ will result in an increase in R_0 by $k\%$. The sensitivity indices of R_0 to the model's parameters are evaluated at the parameter baseline and are displayed in the table below.

S/N	Parameter	Sensitivity index	Comment
1	β_1	$+0.07003$	Enhanced disease spread
2	β_2	$+0.92997$	Enhanced disease spread
3	ρ	$+0.21852$	Enhanced disease spread
4	τ	$+1.50954$	Enhanced disease spread
5	θ	-0.01353	Eradicate disease
6	ϕ_1	-0.04639	Eradicate disease
7	ϕ_2	-0.89208	Eradicate disease
8	γ_1	-0.09924	Eradicate disease
9	γ_2	-0.00007	Eradicate disease

TABLE 2. Sensitivity index.

According to the sensitivity index table, τ is the parameter with the highest degree of sensitivity. Since $\Upsilon_L^{R_0} = 1.50954$, a 10% reduction in τ will result in a 15.092% reduction in R_0. Similarly, a 10% increase in τ will also result in a 15.092% rise in R_0.

Figure 2 presents the normalized forward sensitivity indices of the basic reproduction number with regard to each of the baseline parameter values.

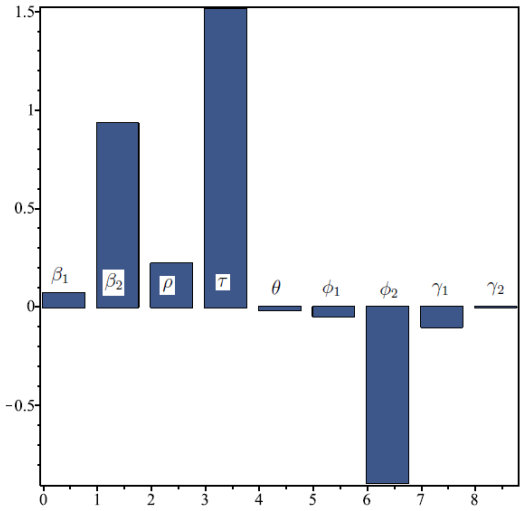

FIGURE 2. Sensitivity indices graph

3.7. **Bifurcation Analysis.** Here, we use Castllo-Chavez and Song [2] to analyze the bifurcation of the model (1). By letting $S(t) = x_1, E(t) = x_2, I_c(t) = x_3, I_r(t) = x_4, T(t) = x_5$ and $R(t) = x_5$ we have

$$
\begin{aligned}
\frac{dx_1}{dt} &= \Lambda - \beta_1 x_1 x_3 - \beta_2 x_1 x_4 + \alpha x_5 - \mu x_1 : f_1,\\
\frac{dx_2}{dt} &= \beta_1 x_1 x_3 + \beta_2 x_1 x_4 - (\tau + \mu) x_2 := f_2,\\
\frac{dx_3}{dt} &= \rho\tau x_2 - (\phi_1 + \theta + \gamma_1 + \mu) x_3 := f_3,\\
\frac{dx_4}{dt} &= (1-\rho)\tau x_2 + \theta x_3 - (\gamma_2 + \phi_2 + \mu) x_4 := f_4,\\
\frac{dx_5}{dt} &= \phi_1 x_3 + \phi_2 x_4 - (\gamma_3 + \epsilon + \mu) x_5 := f_5,\\
\frac{dx_6}{dt} &= \epsilon x_5 - (\alpha + \mu) x_6 := f_6
\end{aligned}
\tag{6}
$$

We will proceed on the assumption that the bifurcation parameter is τ. It follows that, if $R_0 = 1$, then

$$
\tau = \frac{\mu^2 (\phi_2 + \gamma_2 + \mu)(\phi_1 + \theta + \gamma_1 + \mu)}{(\Lambda\rho\beta_1 - \mu^2 - \mu\theta - \mu\gamma_1 - \mu\phi_1)(\phi_2 + \gamma_2 + \mu) - \beta_2 ((\mu + \phi_1 + \gamma_1)\rho - \mu - \theta - \phi_1 - \gamma_1)\Lambda} := \tau^*.
$$

The system of ODEs can be characterized as

$$
x'(t) = f(x, \tau^*)
$$

here the function $f : \mathbb{R}^n \times \mathbb{R}^n$ and is of class C^2, i.e $f \in C^2(\mathbb{R}^n \times \mathbb{R}^n)$. Zero is assumed to be an equilibrium point for the system of differential equations defined above, as well as for all parameter values τ, i.e $f(0, \tau^*) \equiv 0, \forall \tau^* = 0$.

The eigenvalues of characteristic polynomial of system (6), $J(E_0, \tau^*)$ are given as

$$
\lambda_1 = -\mu, \quad \lambda_2 = -(\tau^* + \mu), \quad \lambda_3 = -(\alpha + \mu), \quad \lambda_4 = -(\gamma_3 + \epsilon + \mu)
$$

$$
\lambda_5 = -(\gamma_1 + \gamma_2 + \phi_1 + \phi_2 + 2\mu + \theta), \quad \lambda_6 = 0.
$$

Therefore, the eigenvalue $\lambda_6 = 0$ is a straightforward zero eigenvalue of the matrix $J(E_0, \tau^*,)$ and the other eigenvalues are real and negative.

The right eigenvector that is associated with the zero eigenvalue$\lambda_6 = 0$ is denoted by the symbol $\mathbf{w} = (w_1, w_2, w_3, w_4, w_5, w_6)^T$. This is found as

$$\begin{bmatrix} -\mu & 0 & -\frac{\beta_1\Lambda}{\mu} & -\frac{\beta_2\Lambda}{\mu} & \alpha & 0 \\ 0 & -(\tau^*+\mu) & \frac{\beta_1\Lambda}{\mu} & \frac{\beta_2\Lambda}{\mu} & 0 & 0 \\ 0 & \rho\tau^* & a_1 & 0 & 0 & 0 \\ 0 & \tau^*(1-\rho) & \theta & a_2 & 0 & 0 \\ 0 & 0 & \phi_1 & \phi_2 & a_3 & 0 \\ 0 & 0 & 0 & 0 & \epsilon & -(\alpha+\mu) \end{bmatrix} \begin{bmatrix} w_1 \\ w_2 \\ w_3 \\ w_4 \\ w_5 \\ w_6 \end{bmatrix} = \begin{bmatrix} 0 \\ 0 \\ 0 \\ 0 \\ 0 \\ 0 \end{bmatrix}$$

where $a_1 = -(\phi_1+\theta+\mu+\gamma_1), a_2 = -(\phi_2+\mu+\gamma_2)$ and $a_3 = -(\epsilon+\mu+\gamma_3)$.

This implies $w_1 = -\frac{\Lambda\left(\rho\tau^*\beta_1+\beta_2(\alpha+\mu)\right)}{\mu^2} + \frac{\alpha\mu\left(\phi_2(\alpha+\mu)+\rho\tau^*\phi_1\right)}{\mu^2(\gamma_3+\epsilon+\mu)}$, $w_2 = \phi_1+\gamma_1+\mu+\theta$, $w_3 = \rho\tau^*$, $w_4 = \alpha+\mu$,$w_5 = \frac{\phi_1\rho\tau^*+\phi_2(\alpha+\mu)}{\gamma_3+\epsilon+\mu}$, $w_6 = \epsilon$.

Thus, the right eigenvectors is

$$\mathbf{w} = (w_1, w_2, w_3, w_4, w_5, w_6)^T, \tag{7}$$

where $w_i i, i \cdots 6$ are stated above.

Moreover, the condition $\mathbf{v}\cdot\mathbf{w} = 1$ that is satisfied by the left eigenvector $\mathbf{v} = (v_1, v_2, v_3, v_4, v_5, v_6)$ is given by

$$\begin{bmatrix} v_1, v_2, v_3, v_4, v_5, v_6 \end{bmatrix} \begin{bmatrix} -\mu & 0 & -\frac{\beta_1\Lambda}{\mu} & -\frac{\beta_2\Lambda}{\mu} & \alpha & 0 \\ 0 & -(\tau^*+\mu) & \frac{\beta_1\Lambda}{\mu} & \frac{\beta_2\Lambda}{\mu} & 0 & 0 \\ 0 & \rho\tau^* & a_1 & 0 & 0 & 0 \\ 0 & \tau^*(1-\rho) & \theta & a_2 & 0 & 0 \\ 0 & 0 & \phi_1 & \phi_2 & a_3 & 0 \\ 0 & 0 & 0 & 0 & \epsilon & -(\alpha+\mu) \end{bmatrix} = \begin{bmatrix} 0 \\ 0 \\ 0 \\ 0 \\ 0 \\ 0 \end{bmatrix}$$

$$\begin{cases} -\mu v_1 = 0 \\ -(\tau^*+\mu)v_2 + \rho\tau^* v_3 + (1-\rho)\tau^* v_4 = 0 \\ -\frac{\beta_1\Lambda}{\mu}v_1 + \frac{\beta_1\Lambda}{\mu}v_2 - (\phi_1+\theta+\mu+\gamma_1)v_3 + \theta v_4 + \phi_1 v_5 = 0 \\ -\frac{\beta_2\Lambda}{\mu}v_1 + \frac{\beta_2\Lambda}{\mu}v_2 - (\phi_2+\mu+\gamma_2)v_4 + \phi_2 v_5 = 0 \\ \alpha v_1 - (\epsilon+\mu+\gamma_3)v_5 + \epsilon v_6 = 0 \\ -(\alpha+\mu)v_6 = 0 \end{cases}$$

Solving, we obtain $v_1 = v_5 = v_6 = 0$,

$$v_2 = \frac{\mu(\phi_2+\mu+\gamma_2)}{\beta_2((\rho-1)\tau^*+\mu+\alpha)\Lambda + (\phi_2+\mu+\gamma_2)\mu(2\mu+\tau^*+\theta+\phi_1+\gamma_1)}$$

$$v_3 = \frac{\Lambda\tau^*\beta_2\left(\rho-1\right)+\mu\left(\phi_2+\mu+\gamma_2\right)\left(\tau^*+\mu\right)}{\rho\tau^*\left(\beta_2\left(\left(\rho-1\right)\tau^*+\mu+\alpha\right)\Lambda+\left(\phi_2+\mu+\gamma_2\right)\mu\left(2\mu+\tau^*+\theta+\phi_1+\gamma_1\right)\right)}$$

$$v_4 = \frac{\beta_2\Lambda}{\beta_2\left(\left(\rho-1\right)\tau^*+\mu+\alpha\right)\Lambda+\left(\phi_2+\mu+\gamma_2\right)\mu\left(2\mu+\tau^*+\theta+\phi_1+\gamma_1\right)}.$$

That is

$$\mathbf{v} = (v_1, v_2, v_3, v_4, v_5, v_6) \tag{8}$$

Performing an estimate of the partial derivatives at the disease-free equilibrium, we get the following:

$$\frac{\partial^2 f_1}{\partial x_1\partial x_3} = \frac{\partial^2 f_1}{\partial x_3\partial x_1} = -\beta_1, \frac{\partial^2 f_1}{\partial x_1\partial x_4} = \frac{\partial^2 f_1}{\partial x_4\partial x_1} = -\beta_2, \frac{\partial^2 f_2}{\partial x_1\partial x_3} = \frac{\partial^2 f_2}{\partial x_3\partial x_1} = \beta_1,$$

$$\frac{\partial^2 f_2}{\partial x_1\partial x_4} = \frac{\partial^2 f_2}{\partial x_4\partial x_1} = \beta_2, \frac{\partial^2 f_2}{\partial x_2\partial\tau} = \frac{\partial^2 f_2}{\partial\tau\partial x_2} = -1, \frac{\partial^2 f_3}{\partial x_2\partial\tau} = \frac{\partial^2 f_3}{\partial\tau\partial x_2} = \rho,$$

$$\frac{\partial^2 f_4}{\partial x_2\partial\tau} = \frac{\partial^2 f_4}{\partial\tau\partial x_2} = 1-\rho,$$

while all of the other second-order derivatives fall back to zero.

Determining the coefficients of **a** and **b** according to the definition given in [13] by presuming that f_n is the nth component of f and

$$\mathbf{a} = \sum_{n,i,j=1}^{6} v_n w_i w_j \frac{\partial^2 f_n}{\partial x_i\partial x_j}(E_0, \tau^*)$$

$$\mathbf{b} = \sum_{n,i,j=1}^{6} v_n w_i \frac{\partial^2 f_n}{\partial x_i\partial\tau}(E_0, \tau^*)$$

At the point where x equals zero, the local dynamics of the equation (1) are completely determined by the coefficients **a** and **b.**

The derivatives that are not zero in estimating the co-efficients of **a** and **b** taking into the consideration the systen (6) for the terms $\frac{\partial^2 f_n}{\partial x_i\partial x_j}(E_0, \tau^*)$ and $\frac{\partial^2 f_n}{\partial x_i\partial\tau}(E_0, \tau^*)$ are as follows:

$$\mathbf{a} = 2v_1w_1w_3\frac{\partial^2 f_1}{\partial x_1\partial x_3}(E_0, \tau^*) + 2v_1w_1w_4\frac{\partial^2 f_1}{\partial x_1\partial x_4}(E_0, \tau^*)$$
$$+ 2v_2w_1w_4\frac{\partial^2 f_2}{\partial x_1\partial x_4}(E_0, \tau^*) + 2v_2w_1w_3\frac{\partial^2 f_2}{\partial x_1\partial x_3}(E_0, \tau^*)$$

and

$$\mathbf{b} = v_2w_2\frac{\partial^2 f_2}{\partial x_2\partial\tau}(E_0, \tau^*) + v_3w_2\frac{\partial^2 f_3}{\partial x_2\partial\tau}(E_0, \tau^*) + v_4w_2\frac{\partial^2 f_4}{\partial x_2\partial\tau}(E_0, \tau^*)$$

When we take into account the values that we found for w_i and v_i along with the partial derivatives of the second order that we found in system (6), Since $v_1 = 0$ it then follows that

$$\mathbf{a} = 2v_2w_1w_4\beta_2 + 2v_2w_1w_3\beta_1$$

and

$$\mathbf{b} = -v_2 w_2 + v_3 w_2 \rho + v_4 w_2 (1-\rho)$$
$$\mathbf{a} = -\frac{(\phi_2 + \mu + \gamma_2)(\rho\tau\beta_1 + \alpha\beta_2 + \mu\beta_2) H}{\mu(\gamma_3 + \epsilon + \mu) G} > 0$$

where

$$H = (-\alpha\mu(\phi_2(\alpha+\mu) + \tau\rho\phi_1) + \Lambda(\rho\tau\beta_1 + \alpha\beta_2 + \mu\beta_2)(\gamma_3 + \epsilon + \mu))$$
$$G = \mu^3 + A\mu^2 + \left(\frac{\beta_2\Lambda}{2} + \frac{(\phi_2+\gamma_2)(\tau+\theta+\gamma_1+\phi_1)}{2}\right)\mu + \frac{((\rho-1)\tau+\alpha)\beta_2\Lambda}{2}$$

and

$$A = \frac{\gamma_1}{2} + \gamma_2 + \frac{\tau}{2} + \frac{\theta}{2} + \frac{\phi_1}{2} + \phi_2$$
$$\mathbf{b} = \frac{(\rho-1)\mu^3 + a_{11}\mu^2 + a_{12}\mu - \Lambda\beta_2(\rho-1)(-\rho\tau+\theta+\gamma_1+\phi_1)}{2\mu^3 + a_{13}\mu^2 + a_{14}\mu + \Lambda\beta_2(\rho\tau+\alpha-\tau)} < 0$$
$$a_{11} = ((\gamma_2+\tau+\phi_2)\rho - \gamma_1 - \gamma_2 - \theta - \phi_1 - \phi_2)$$
$$a_{12} = (-\Lambda(\rho-1)\beta_2 - (\phi_2+\gamma_2)(-\rho\tau+\theta+\gamma_1+\phi_1))$$
$$a_{13} = (\gamma_1 + 2\gamma_2 + \tau + \theta + \phi_1 + 2\phi_2)$$
$$a_{14} = (\beta_2\Lambda + (\phi_2+\gamma_2)(\tau+\theta+\gamma_1+\phi_1))$$

The coefficient of **a** is found to be positive, whereas the coefficient of **b** is found to be negative. If **a** is strictly higher than zero and **b** is rigorously less than zero, and τ^* is strictly less than zero, then the system is unstable, and there exists a negative and locally asymptotically stable negative equilibrium, as stated by [13].

4. Numerical Simulation and Results

For the output of the present model, we solve numerical using fourth order Runge-Kuta method and simulate using Maple with DEplots packages. The susceptible, exposed, careless infective, careful infective, treatment and recoverred at the moment of the initial $t = 0$ are listed respectively: $S(0) = 0.4, E(0) = 0.3, I_c(0) = 0.2, I_r(0) = 0.1, T(0) = 0$ and $R(0) = 0$. The following set of figures presents the findings that obtained from running a numerical simulation.

Parameter	Values, Units	Source
β_1	0.0805,day^{-1}	[4]
β_2	0.041,day^{-1}	Assumed
α	0.07143,day^{-1}	Assumed
Λ	0.02537,day^{-1}	[4]
θ	0.445,day^{-1}	Assumed
μ	0.0106,day^{-1}	[14]
ρ	0.0668,day^{-1}	[14]
τ	$1/7$,day^{-1}	[15]
γ_1	0.1945×10^{-4},day^{-1}	[14]
γ_2	0.1945×10^{-4},day^{-1}	[14]
γ_3	0.1945×10^{-4},day^{-1}	[14]
ϕ_1	0.25,day^{-1}	[14]
ϕ_2	0.25,day^{-1}	[14]
ϵ	0.0766169,day^{-1}	[4]

TABLE 3. Estimated model parameters

The impact of the scenario is examined in figure 3, which reveals that the susceptible compartment grows after a certain number of days, whereas the exposed compartment gradually shrinks and the careful infective compartment increasses for the first few days and after which it decreases. During the first few days, the number of people in the careless compartment falls while the number of people in the treatment compartment increases. In the meantime, as the days pass, people are beginning to recover. The results of increasing the transmission rate with careless infective β_1 are displayed in figures for each compartment, and they can be seen below (4-8). Figure 4 illustrates how a susceptible population can be reduced when there is an increase in the transmission rate caused by careless infective behavior. This indicates that a greater number of people are becoming infected with COVID-19, while fig.5 demonstrates an increase in the rate of transmission that occurs when careless infectious behavior leads to an expansion of the population in an exposed compartment. As can be seen in fig.6, an increase in β initially does not have any effect on the careful infective compartment; however, as time passes, it is observed that this change does improve the careful compartment. As shown in fig.7, as β_1 rise, an increasing number of people become infected and progress to the treatment compartment. In the beginning, things were different, but as time went on, the population of

the compartment increased. As shown in fig.8, the number of people who are able to recover from COVID-19 increases proportionally with the rising β_1 shortly after few days.

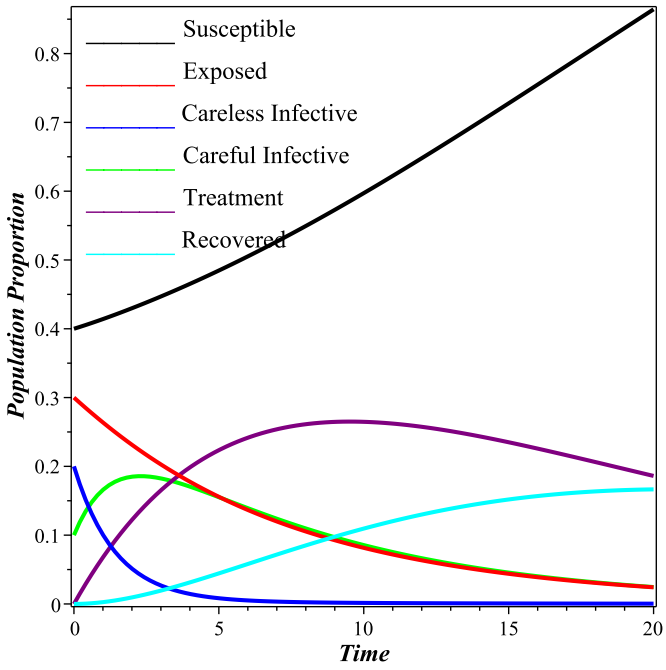

FIGURE 3. Dynamic of the six compartments.

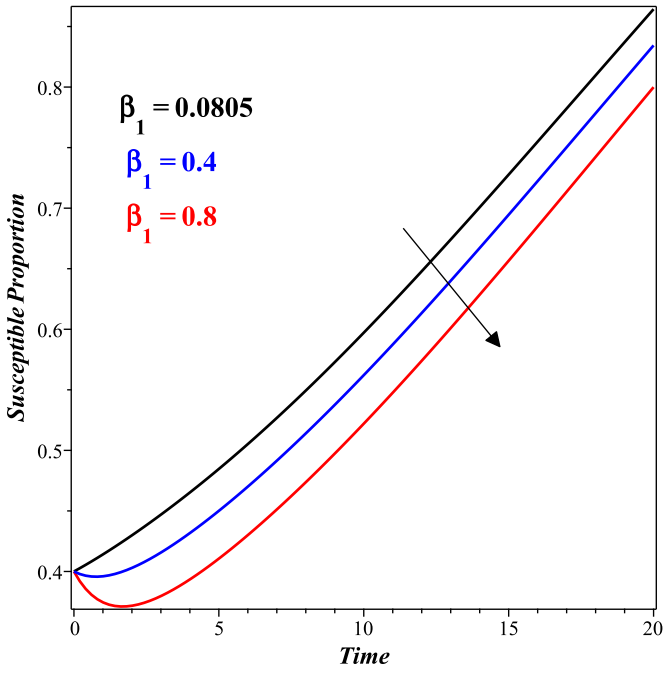

FIGURE 4. Behaviour of Susceptible as β_1 increases

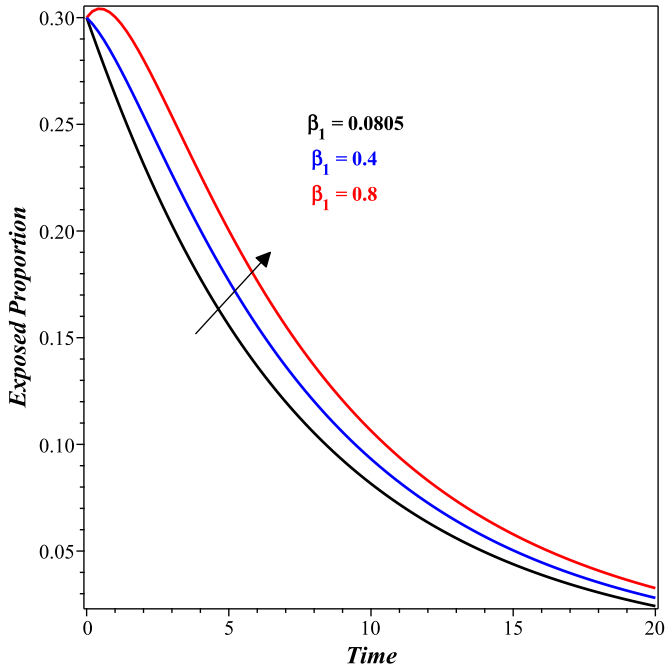

FIGURE 5. Behaviour of exposed as β_1 increases

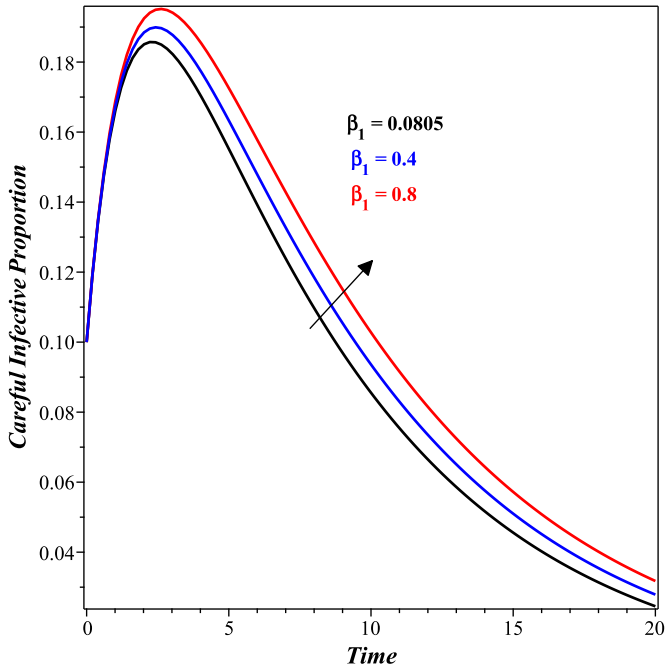

FIGURE 6. Behaviour of careful infective as β_1 increases

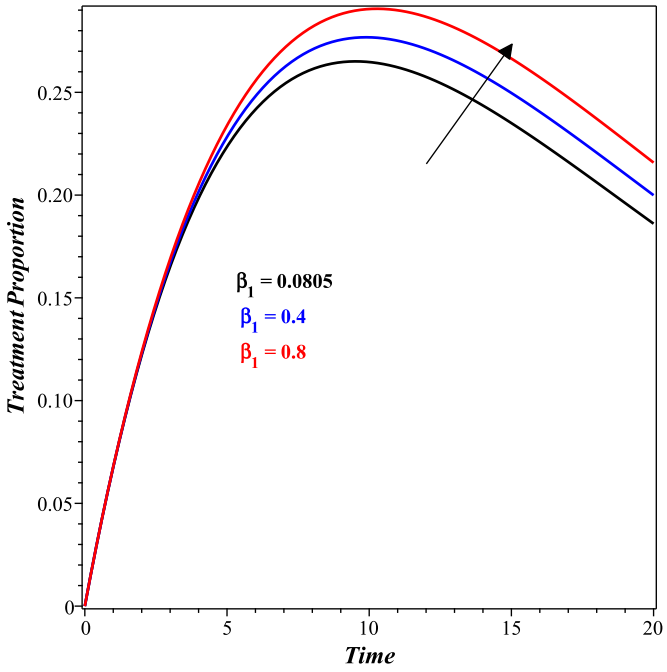

FIGURE 7. Behaviour of treatment as β_1 increases

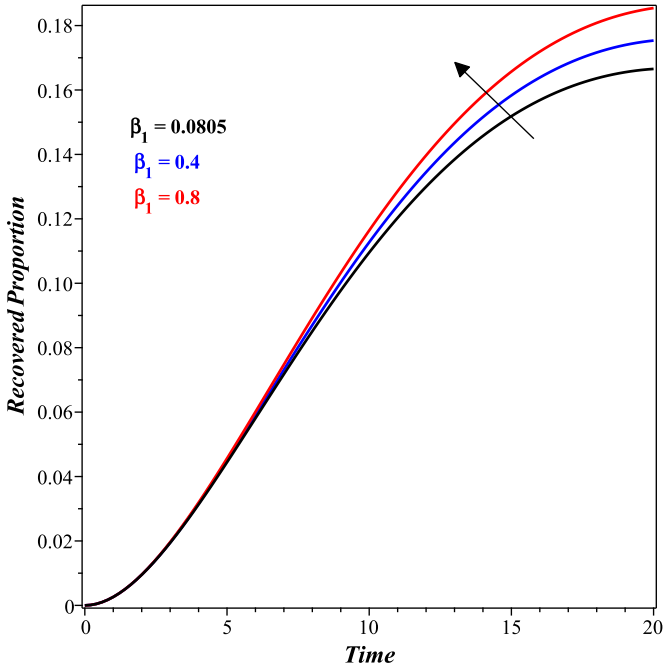

FIGURE 8. Behaviour of recovered as β_1 increases

The effects that the treatment rate of careless and careful infective ϕ_1 and ϕ_2 have on each of the compartments are depicted in figures 9-14. Fig.9 illustrates that an increase in the treatment rate for both careless and careful infectives ϕ_1 and ϕ_2 leads to an increase in the number of susceptible individuals. This suggests that as the rates are increasing, a greater proportion of infected individuals are being treated, which in turn leads to a decrease in the number of individuals in the infected compartments, as shown in figures 11 and 12. However, there is no guarantee that the number of individuals who are susceptible will decrease even if treatment rates are increased. This is due to the fact that treating those who are already infected does not have an immediate impact on the total population of susceptible people. Fig.10 shows the implicaion of increasing ϕ_1 and ϕ_2 on the exposed compartment. Increasing ϕ_1 and ϕ_2 lead to a decrease in the number of individuals in the infeced compartment, which ultimately resulted in a reduction in the number of individuals entering the exposed compartment. If a greater number of infected individuals receive treatment, it is possible that they will become less infectious and will have a lower risk of transmitting the COVID-19 disease.This may reduce the likelihood of exposing susceptible individuals to the COVID-19 disease and, consequently reduce the number of individual entering the exposed compartment. The effects of increasing the ϕ_1 and ϕ_2 on the treatment compartment are depicted in Fig.13. If the number of people who are infected is high, increasing ϕ_1 and ϕ_2 will result in a larger treatment compartment. On the other hand, if the number of people who are infected is low, increasing the ϕ_1 and ϕ_2 will result in a smaller treatment compartment, as shown in Figure 13. The effects of ϕ_1 and ϕ_2 on the recovery compartment are represented graphically in Fig.14. As ϕ_1 and ϕ_2 continue to rise, so does the the rocovery compartment, as can be seen in Fig.14.Increasing the treatment rates help infected individuals to recover more quickly from the COVID-19 disease. The treatment lessens the severity of the COVID-19, shortens the duration, and relieves the symptoms of the illness; as a result, patients are able to recover from it more quickly.

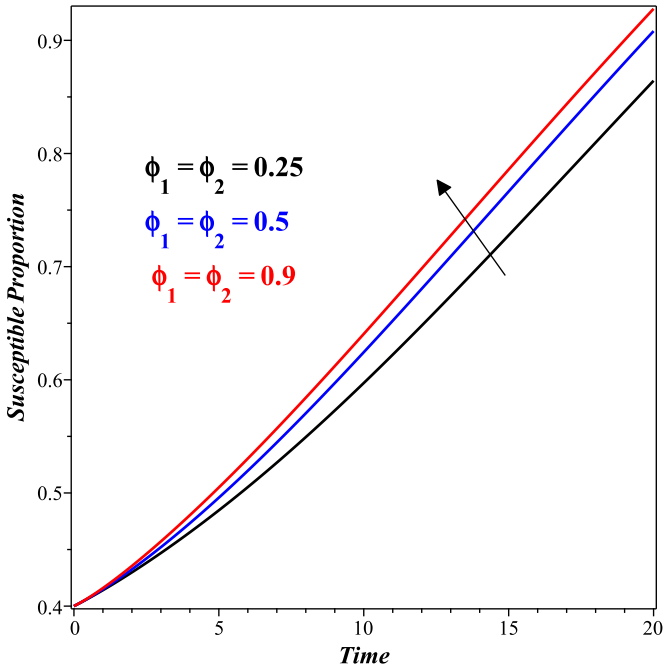

FIGURE 9. Behaviour of Susceptible as ϕ_1 and ϕ_2 increase

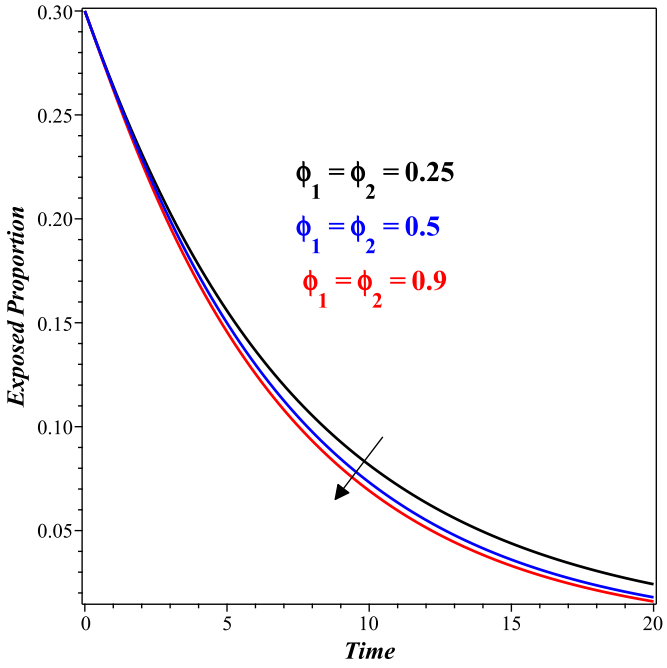

FIGURE 10. Behaviour of exposed as ϕ_1 and ϕ_2 increase

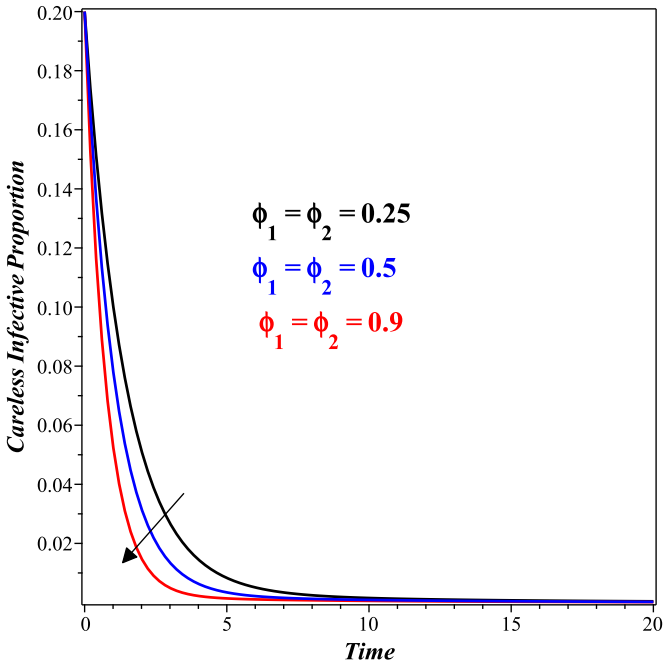

FIGURE 11. Behaviour of careless infective as ϕ_1 and ϕ_2 increase

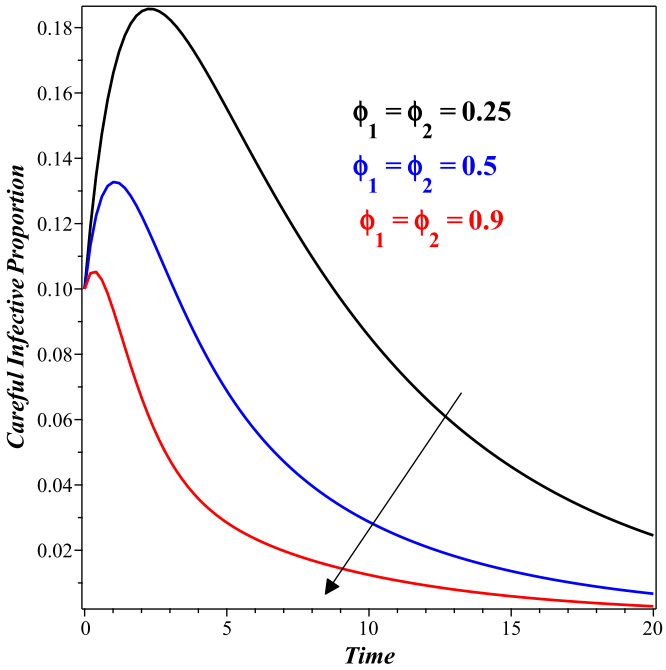

FIGURE 12. Behaviour of careful infective as ϕ_1 and ϕ_2 increases

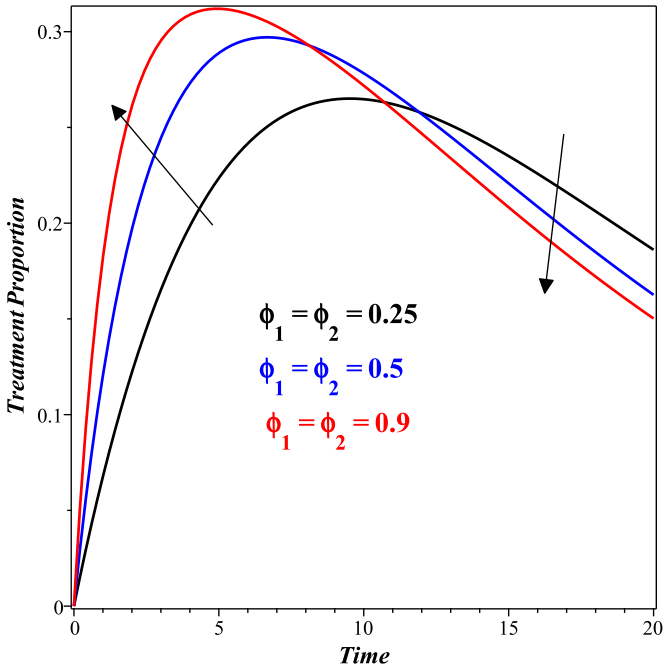

FIGURE 13. Behaviour of treatment as ϕ_1 and ϕ_2 increase

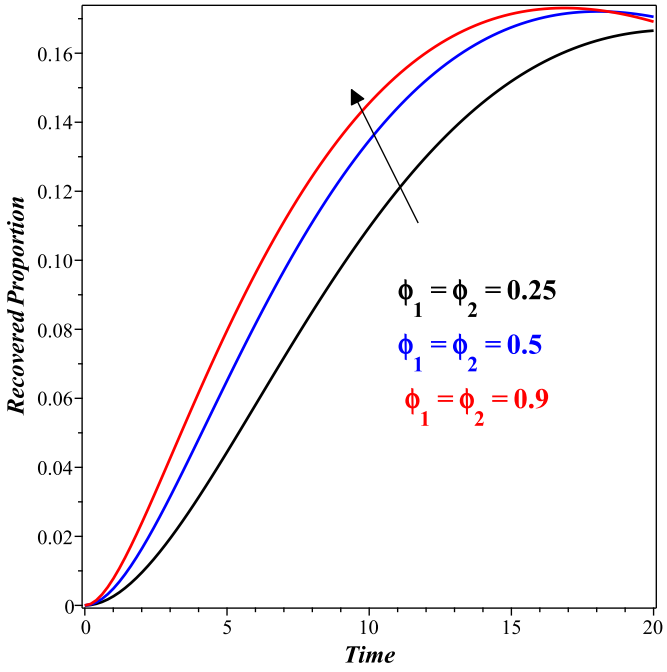

FIGURE 14. Behaviour of recovered as ϕ_1 and ϕ_2 increase

5. Conclusion

In order to model the dynamics of COVID-19, we considered a system of differential equations, with a particular emphasis on careless and careful infectives. We perform the positivity and boundedness on the model, as well as estimate the basic reproduction number for the formulated model. The local and global stabilities analysis, sensitivity analysis, and bifurcation analysis for the models were all carried out. To investigate the effect that β_1, ϕ_1 and ϕ_2 have on the various compartments, we carried out a numerical simulation. The transmission rate with careless infective β_1 increases the exposured, careful infective, treatment, and recovery compartments, according to the numerical results that we obtained. whereas the exposed, careless infective, and careful infective compartments are reduced by treatment rates $\phi_1$and ϕ_2, respectively.

References

[1] U. Avila-Ponce de León, Á.G.C. Pérez, E. Avila-Vales, An SEIARD epidemic model for COVID-19 in Mexico: Mathematical analysis and state-level forecast, Chaos Solitons Fractals. 140 (2020), 110165. https://doi.org/10.1016/j.chaos.2020.110165.

[2] A.S. Eegunjobi, O.D. Makinde, Mathematical analysis of two strains of Covid-19 using SEIR model, J. Math. Fund. Sci. 54 (2022), 211-232.

[3] D. Okuonghae, A. Omame, Analysis of a mathematical model for COVID-19 population dynamics in Lagos, Nigeria, Chaos Solitons Fractals. 139 (2020), 110032. https://doi.org/10.1016/j.chaos.2020.110032.

[4] I. Ahmed, G.U. Modu, A. Yusuf, et al. A mathematical model of Coronavirus Disease (COVID-19) containing asymptomatic and symptomatic classes, Results Phys. 21 (2021), 103776. https://doi.org/10.1016/j.rinp.2020.103776.

[5] N. Scott, A. Palmer, D. Delport, et al. Modelling the impact of relaxing (COVID-19) control measures during a period of low viral transmission, Med. J. Australia. 214 (2020), 79-83. https://doi.org/10.5694/mja2.50845.

[6] Y. Zou, S. Pan, P. Zhao, et al. Outbreak analysis with a logistic growth model shows COVID-19 suppression dynamics in China, PLoS ONE. 15 (2020), e0235247. https://doi.org/10.1371/journal.pone.0235247.

[7] A.M.C.H. Attanayake, S.S.N. Perera, S. Jayasinghe, Phenomenological modelling of COVID-19 epidemics in Sri Lanka, Italy, the United States, and Hebei Province of China, Comput. Math. Methods Med. 2020 (2020), 6397063. https://doi.org/10.1155/2020/6397063.

[8] K. Roosa, Y. Lee, R. Luo, et al. Real-time forecasts of the COVID-19 epidemic in China from February 5th to February 24th, 2020, Infect. Dis. Model. 5 (2020), 256-263. https://doi.org/10.1016/j.idm.2020.02.002.

[9] Z.Y. Zhao, Y.Z. Zhu, J.W. Xu, et al. A five-compartment model of age-specific transmissibility of SARS-CoV-2, Infect. Dis. Poverty. 9 (2020), 117. https://doi.org/10.1186/s40249-020-00735-x.

[10] P. Samui, J. Mondal, S. Khajanchi, A mathematical model for COVID-19 transmission dynamics with a case study of India, Chaos Solitons Fractals. 140 (2020), 110173. https://doi.org/10.1016/j.chaos.2020.110173.

[11] K. Sadri, H. Aminikhah, M. Aminikhah, A mathematical system of COVID-19 disease model: Existence, uniqueness, numerical and sensitivity analysis, MethodsX. 10 (2023), 102045. https://doi.org/10.1016/j.mex.2023.102045.

[12] A. Zeb, E. Alzahrani, V.S. Erturk, G. Zaman, Mathematical model for coronavirus disease 2019 (COVID-19) containing isolation class, BioMed Res. Int. 2020 (2020), 3452402. https://doi.org/10.1155/2020/3452402.

[13] C. Castillo-Chavez, B. Song, Dynamical models of tuberculosis and their applications, Math. Biosci. Eng. 1 (2004), 361-404.

[14] S. Khajanchi, K. Sarkar, J. Mondal, K.S. Nisar, S.F. Abdelwahab, Mathematical modeling of the COVID-19 pandemic with intervention strategies, Results Phys. 25 (2021), 104285. https://doi.org/10.1016/j.rinp.2021.104285.

[15] D. Cucinotta, M. Vanelli, WHO declares COVID-19 a pandemic, Acta Biomedica. 91 (2020), 157-160. https://doi.org/10.23750/abm.v91i1.9397.

[16] B. Seidu, C.S. Bornaa, O.D. Makinde, An Ebola model with hyper-susceptibility, Chaos Solitons Fractals. 138 (2020), 109938. https://doi.org/10.1016/j.chaos.2020.109938.

[17] A.S. Eegunjobi, M.C. Anyanwu, S.N. Neossi-Nguetchue, Modelling the super-infection of two strains of dengue virus, J. Egypt. Math. Soc. 31 (2023), 1. https://doi.org/10.1186/s42787-023-00161-6.

[18] G.T. Tilahun, O.D. Makinde, D. Malonza, Co-dynamics of Pneumonia and Typhoid fever diseases with cost effective optimal control analysis, Appl. Math. Comput. 316 (2018), 438-459. https://doi.org/10.1016/j.amc.2017.07.063.

[19] I. Takaidza, O.D. Makinde, O.K. Okosun, Computational modelling and optimal control of ebola virus disease with non-linear incidence rate, J. Phys.: Conf. Ser. 818 (2017), 012003. https://doi.org/10.1088/1742-6596/818/1/012003.

[20] G.T. Tilahun, O.D. Makinde, D. Malonza, Modelling and optimal control of pneumonia disease with cost-effective strategies, J. Biol. Dyn. 11 (2017), 400-426. https://doi.org/10.1080/17513758.2017.1337245.